**Original Article** | Neuroimaging and Head & Neck

http://dx.doi.org/10.3348/kjr.2014.15.6.810
pISSN 1229-6929 · eISSN 2005-8330
Korean J Radiol 2014;15(6):810-816

Korean Journal of Radiology
KJR

# Is Diffusion-Weighted MRI Useful for Differentiation of Small Non-Necrotic Cervical Lymph Nodes in Patients with Head and Neck Malignancies?

Hyun Kyung Lim, MD[1, 2], Jeong Hyun Lee, MD[1], Hye Jin Baek, MD[1], Namkug Kim, PhD[1], Hayoung Lee, MD[1], Jee Won Park, MD[1], Sang Yoon Kim, MD[3], Kyung Ja Cho, MD[4], Jung Hwan Baek, MD[1]

[1]Department of Radiology and Research Institute of Radiology, Departments of [3]Otolaryngology, and [4]Pathology, Asan Medical Center, University of Ulsan College of Medicine, Seoul 138-736, Korea; [2]Department of Radiology, Soonchunhyang University Hospital, Seoul 140-743, Korea

**Objective:** To evaluate the usefulness of measuring the apparent diffusion coefficient (ADC) in diffusion-weighted magnetic resonance imaging to distinguish benign from small, non-necrotic metastatic cervical lymph nodes in patients with head and neck cancers.

**Materials and Methods:** Twenty-six consecutive patients with head and neck cancer underwent diffusion-weighted imaging (b value, 0 and 800 s/mm$^2$) preoperatively between January 2009 and December 2010. Two readers independently measured the ADC values of each cervical lymph node with a minimum-axial diameter of ≥ 5 mm but < 11 mm using manually drawn regions of interest. Necrotic lymph nodes were excluded. Mean ADC values were compared between benign and metastatic lymph nodes after correlating the pathology.

**Results:** A total of 116 lymph nodes (91 benign and 25 metastatic) from 25 patients were included. Metastatic lymph nodes (mean ± standard deviation [SD], 7.4 ± 1.6 mm) were larger than benign lymph nodes (mean ± SD, 6.6 ± 1.4 mm) ($p$ = 0.018). Mean ADC values for reader 1 were 1.17 ± 0.31 x $10^{-3}$ mm$^2$/s for benign and 1.25 ± 0.76 x $10^{-3}$ mm$^2$/s for metastatic lymph nodes. Mean ADC values for reader 2 were 1.21 ± 0.46 x $10^{-3}$ mm$^2$/s for benign and 1.14 ± 0.34 x $10^{-3}$ mm$^2$/s for metastatic lymph nodes. Mean ADC values between benign and metastatic lymph nodes were not significantly different ($p$ = 0.594 for reader 1, 0.463 for reader 2).

**Conclusion:** Measuring mean ADC does not allow differentiating benign from metastatic cervical lymph nodes in patients with head and neck cancer and non-necrotic, small lymph nodes.

**Index terms:** *Diffusion weighted imaging; Metastasis; Head and neck cancer; Lymph node*

## INTRODUCTION

Lymph node metastasis is an important prognostic factor in patients with head and neck squamous cell carcinoma (HNSCC). An accurate assessment of lymph node metastasis is an important prerequisite for staging and proper treatment planning. Computed tomography (CT) and/or magnetic resonance imaging (MRI) are frequently used to preoperatively assess lymph node status in patients with HNSCC using morphologic criteria (1-6). Among them, size-related criteria offer the easiest way to assess malignancy with high reproducibility and a wide range of diagnostic sensitivities and specificities depending on the cut-off value used. Van den Brekel et al. (2) reported that a minimum axial diameter > 11 mm showed very high specificity (95–100%) in a CT scan study.

The presence of central necrosis is considered the most reliable and specific finding suggesting nodal metastasis

Received June 7, 2013; accepted after revision July 21, 2014.
**Corresponding author:** Jeong Hyun Lee, MD, Department of Radiology and Research Institute of Radiology, Asan Medical Center, University of Ulsan College of Medicine, 88 Olympic-ro 43-gil, Songpa-gu, Seoul 138-736, Korea.
• Tel: (822) 3010-4352 • Fax: (822) 476-4719
• E-mail: jeonghlee@amc.seoul.kr

Korean Journal of Radiology
KJR

(1, 4, 5). However, CT and MRI may fail to depict areas of necrosis < 3 mm and are unable to distinguish tumor necrosis from other elements of malignant nodes (4). This finding suggests that assessing nodal status in patients with HNSCC depending on morphological criteria is limited considering the clinical significance of nodal status for determining patient prognosis. These problems are not always solved by [$^{18}$F]-fluorodeoxyglucose positron emission tomography, for which the main diagnostic limitations include lower spatial resolution and lower specificity due to the false-positive uptake of reactive lymph node hyperplasia (7, 8).

An increasing number of studies have reported the ability of diffusion-weighted imaging (DWI) to distinguish benign from metastatic lymph nodes in patients with head and neck cancer (9-15). The main advantage of DWI is its sensitivity to microscopic pathological alterations before they become visible on conventional MRI; thus, DWI could remedy the morphological criteria limitations. Except for a study by Sumi et al. (10), metastatic lymph nodes have consistently been described with significantly lower apparent diffusion coefficient (ADC) values (0.59–1.09 x $10^{-3}$ $mm^2/s$) than those of benign lymph nodes (1.21–1.64 x $10^{-3}$ $mm^2/s$) (9, 11-13, 16). DWI distinguishes benign from metastatic lymph nodes with sensitivities of 84–100% and specificities of 84–94% with different ADC thresholds of 0.94–1.38 x $10^{-3}$ $mm^2/s$. The contradicting results of the study by Sumi et al. may be related to inclusion of a high number of necrotic metastases (up to 48%). DWI was superior to conventional MRI for nodal staging of HNSCC in a recent meta-analysis (17).

However, no study has investigated the added value of ADC measurements using DWI to diagnose nodal metastasis in patients with HNSCC by focusing on small non-necrotic lymph nodes. Therefore, we investigated the usefulness of ADC measurements to assess cervical lymph nodes showing no specific signs of metastasis, including central necrosis or an increased minimum axial diameter > 11 mm to detect metastasis in patients with HNSCC.

## MATERIALS AND METHODS

This retrospective study was approved by our Institutional Review Board for human investigation, and informed consent was waived.

### Patients and Lymph Node Selection

We initially included 26 consecutive patients with biopsy-proven HNSCC between January 2009 and December 2010, who had undergone a head and neck MRI examination as well as surgical treatment, including neck dissection, within 1 month following their MRI examination. None of these patients underwent preoperative chemotherapy or radiotherapy.

Two head and neck radiologists, who were blinded to the clinical and surgical information, reviewed the T1-, T2-, and contrast-enhanced T1-weighted images with consensus regarding lymph node size and the presence of necrosis. Lymph node size for the ADC measurements was set at a minimum axial diameter of 5 mm to reduce the effects of partial volume artifacts. Lymph nodes with a central, non-enhancing area suggesting necrosis or those > 11 mm in minimum axial diameter were excluded.

Among the 135 lymph nodes fulfilling the size criteria, 11 were excluded due to central necrosis. One patient with eight lymph nodes was excluded due to poor DWI image quality. Therefore, 116 lymph nodes in 25 patients (mean ± standard deviation [SD] age, 55 ± 13 years; range, 25–84 years; female/male, 17/8) were finally included in our study. The mean ± SD time interval between MRI examination and surgery was 12 ± 8 days (range, 1–29 days). The locations of the primary tumors and the pathologic nodal staging are shown in Table 1.

### MRI Examinations

Magnetic resonance imaging was obtained on a 1.5-T MR scanner (Achieva, Philips Medical Systems, Best, the Netherlands or Intera, Philips Medical Systems) (n = 16) or on a 3-T MR scanner (Achieva, Philips Medical Systems) (n = 9) using a 16-channel neurovascular coil (SENSE NV coil, Philips Medical Systems). Among the 116 lymph nodes, 25 (22 benign and three malignant) were imaged with the 1.5-T MR scanner, and 91 lymph nodes (69 benign and 22 malignant) were imaged with the 3-T MR scanner. A transverse T2-weighted turbo spin-echo (TSE) sequence was performed with a repetition time (TR)/echo time (TE) of 3090/100 ms, acquisition time of 2 minutes 22 seconds

**Table 1. Locations of Primary Tumors and Pathologic Nodal Stages of Enrolled Patients**

| Location of Primary Tumors | | Pathologic Nodal Stages | |
|---|---|---|---|
| Tongue | 22 | N0 | 13 |
| Buccal mucosa | 1 | N1 | 4 |
| Gingiva | 1 | N2b | 4 |
| Pyriform sinus | 1 | N2c | 4 |

**Note.**— Values are number of patients.

for the 1.5-T MR scanner and with a TR/TE of 3906/100 ms, acquisition time of 2 minutes 59 seconds for the 3-T MR scanner. A transverse T1-weighted TSE sequence was performed with a TR/TE of 615/10 ms, acquisition time of 2 minutes and 20 seconds for the 1.5-T MR scanner and a TR/TE of 675/10 ms, acquisition time of 2 minutes and 51 seconds for the 3-T MR scanner. 1.5-T MR images were obtained with field of view (FOV) of 180 (anterior to posterior [AP]) x 180 (right to left [RL]) x 120 (feet to head [FH]) mm, reconstruction voxels of 0.35 x 0.35 x 4.00 mm. 3-T MR was performed with an FOV of 190 (AP) x 190 (RL) x 120 (FH) mm, reconstruction voxels of 0.37 x 0.37 x 4.00 mm. All T1- and T2-weighted images were acquired with 30 sections, 4-mm section thickness without a gap, and a reconstructed matrix of 512. Intravenous gadobenate dimeglumine (MultiHance: Bracco Diagnostics, Milan, Italy) was injected in all patients to obtain post-contrast T1-weighted images.

Diffusion-weighted imaging scans of the head and neck were obtained using single-shot, echo-planar imaging in the transverse plane before contrast injection. The applied sequence parameters for DWI on the 1.5-T MR scanner were: TR/TE/inversion time (TI) of 4188/69/160 ms; number of slices, 60; slice thickness/gap, of 4/0 mm; FOV of 235 (AP) x 300 (RL) x 240 mm (FH); reconstruction matrix of 256; echo train length of 37; bandwidth of 2293.1 Hz; b values of 0 and 800 s/mm$^2$; parallel imaging (sensitivity encoding [SENSE] factor of 2); actual voxel size of 2.68 x 3.40 x 4.00 mm; reconstructed voxel size of 1.17 x 1.18 x 4.00 mm; and an image acquisition time of 2 minutes and 24 seconds. The applied sequence parameters for DWI on the 3-T MR scanner were: TR/TE/TI of 10976/50/260 ms; number of slices, 50; slice thickness/gap of 4/0 mm; FOV of 240 (AP) x 240 (RL) x 200 mm (FH); reconstruction matrix of 432; echo train length of 33; bandwidth of 1780.3 Hz; b values of 0 and 800 s/mm$^2$; parallel imaging (SENSE factor of 4); actual voxel size of 2.00 x 1.94 x 4.00 mm; reconstructed voxel size of 0.56 x 0.56 x 4.00 mm; and image acquisition time of 5 minutes and 18 seconds. The diffusion gradients were applied in three orthogonal directions (x, y, z).

### ADC Measurements

Two neuroradiologists, who were blinded to both the TSE imaging findings and the clinical data, independently analyzed the DW images. Reader 1 was a faculty radiologist in the neuroradiology division, who had interpreted at least 1000 head and neck MRI examinations over 8 years; reader 2 was a fellow neuroradiologist, who had interpreted approximately 150 head and neck MRI examinations images over 6 years. The ADC measurements were determined 1 month after selecting the lymph node to minimize bias. The MRI data were transferred to DiffusionLab™ commercial software (Clinical Imaging Solution Inc., Seoul, Korea) for ADC measurements, and the regions of interest (ROI) were drawn freehand over the lymph nodes, containing the entire lymph node volume at every section identified on the b value of 800 s/mm$^2$ images. The mean ADC value and ROI volume were automatically calculated by combining the b values of 0 and 800 s/mm$^2$ images.

### Topographic Correlation of Lymph Nodes

The reference standards were the neck dissection surgical and pathology reports. The lymph nodes were excised en bloc along with adjacent reference structures, including muscles, salivary gland, and veins to ensure the exact nodal station. A node-by-node correlation was done between the MRI and the surgical specimens. To ensure that the lymph node obtained by neck dissection was the same node as that seen on MRI, the nodal station and its size were matched with consensus between MRI and the pathology by two authors. Final decisions regarding the correlation were reached by consensus between a radiologist and a pathologist. All lymph nodes matched clearly between the imaging and pathology, and none of those lymph nodes were excluded from the analysis. The histopathological and radiological findings were correlated after all image analysis was completed.

### Statistical Analysis

Statistical analyses were performed using SPSS 19.0 software (SPSS Inc., Chicago, IL, USA). Numerical data are reported as mean ± SD. The independent two-sample *t* test was performed to compare the minimum axial diameters of benign and metastatic lymph nodes and also to compare mean ADC values of benign and metastatic lymph nodes measured separately by each reader. The paired *t* test was used to separately compare the measured ADC values of the benign and metastatic lymph nodes between the two readers. To ensure that there was no difference in the ROI measurements between the two readers, we separately compared mean ROI volumes between the readers using the paired *t* test for benign and metastatic lymph nodes. A $p$ value < 0.05 was considered significant. We also evaluated inter-observer agreement between the two readers regarding

Korean Journal of Radiology
KJR

**Table 2. ADC Value of Benign and Metastatic Lymph Nodes as Assessed by Two Readers**

| | Benign LNs (n = 91) | Metastatic LNs (n = 25) | *P* |
|---|---|---|---|
| Reader 1 | 1.17 ± 0.31 x $10^{-3}$ | 1.25 ± 0.76 x $10^{-3}$ | 0.594 |
| Reader 2 | 1.21 ± 0.46 x $10^{-3}$ | 1.14 ± 0.34 x $10^{-3}$ | 0.463 |

**Note.**— Values are presented as mean ± standard deviation ($mm^2/s$). ADC = apparent diffusion coefficient, LN = lymph node

the measured ADC values and the ROI volumes using the intraclass correlation coefficient (ICC) and interpreted it as follows: poor (0–0.2), fair (0.3–0.4), moderate (0.5–0.6), strong (0.7–0.8), and almost perfect (> 0.8) (18).

## RESULTS

A total of 116 lymph nodes (91 benign and 25 metastatic) from 25 patients were finally included in this study. The mean minimum axial diameter was greater in metastatic lymph nodes (mean ± SD, 7.4 ± 1.6 mm; range, 5.0–10.9 mm) than that in benign lymph nodes (mean ± SD, 6.6 ± 1.4 mm; range, 5.2–11.0 mm) ($p$ = 0.018).

No significant difference in the mean ADC values was observed between benign and metastatic cervical lymph nodes, as determined by the two readers ($p$ = 0.594 for reader 1 and 0.463 for reader 2) (Table 2). Figure 1 is a box-and-whisker plot of the benign and metastatic lymph nodes ADC values, as determined by the two readers.

No significant differences were observed in mean ROI volume between the two readers ($p$ = 0.110 for benign lymph nodes and 0.107 for malignant lymph nodes) (Table 3). Inter-observer agreement between the two readers was moderate for the measured ADC values (ICC = 0.530; 95% confidence interval [CI], 0.320–0.675) and almost perfect for the ROI volumes (ICC = 0.964; 95% CI, 0.947–0.975). Figures 2 and 3 show representative cases of metastatic lymph nodes with relatively low and high mean ADC values, respectively.

## DISCUSSION

In this study, we compared mean ADC values of benign and metastatic lymph nodes in patients with HNSCC, targeting small, non-necrotic lymph nodes of minimum axial diameter < 11 mm with manually drawn ROIs. We found that the mean ADC values of the two groups were not significantly different. This result indicates that ROI measurements of mean ADC values did not distinguish benign from metastatic lymph nodes among small, non-necrotic lymph nodes in patients with HNSCC.

The purpose of this study was to evaluate the role of

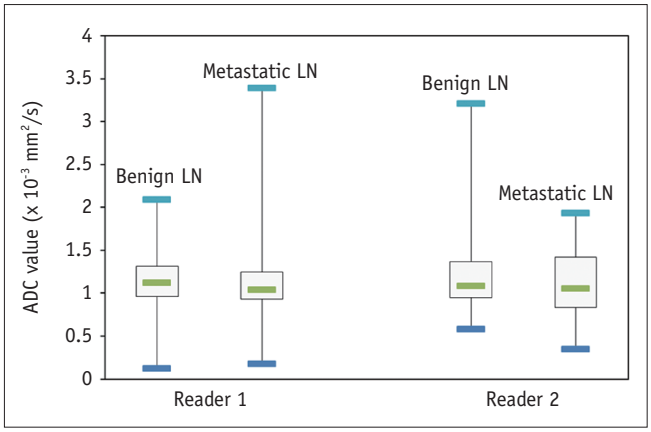


**Fig. 1. Box-and-whisker plot of measured ADC values for benign and metastatic lymph nodes as assessed by two readers.** ADC = apparent diffusion coefficient, LN = lymph node

ADC measurements using DWI to diagnose nodal metastasis in lymph nodes without specific morphological signs of metastasis, such as increased minimum axial diameter or central necrosis. Although a study has evaluated the value of ADC measurements of subcentimeter-sized lymph nodes, the authors did not mention whether central necrotic lymph nodes were excluded or not from their study (9). Previous studies have reported that DWI is superior to conventional MRI for nodal staging of head and neck cancer, and they analyzed the ADC values of lymph nodes with necrosis in the solid portion to distinguish cervical lymph nodes in patients with head and neck cancer (9, 12). An increased minimum axial diameter > 11 mm and central necrosis are highly specific imaging criteria for nodal metastasis in patients with HNSCC. Therefore, in a case of definitely enlarged or necrotic lymph nodes in a patient with HNSCC, an ADC measurement using DWI is not necessary to distinguish benign from metastatic lymph nodes. Small lymph nodes, i.e., < 11 mm in the minimum axial diameter, without necrosis remain a diagnostic dilemma when staging patients with head and neck cancer. Therefore, we attempted to investigate whether ADC measurements could increase the diagnostic ability of MRI to differentiate benign from metastatic lymph nodes of small size and non-necrotic appearance in this study.

Diffusion-weighted imaging is an MRI technique that measures the motion of water molecules in the extracellular,

**Table 3. ROI Volume of Benign and Metastatic Lymph Nodes as Assessed by Two Readers**

| | Benign LNs (n = 91) | Metastatic LNs (n = 25) | *P* |
|---|---|---|---|
| Reader 1 | 1.63 ± 0.86 | 2.10 ± 1.75 | 0.211 |
| Reader 2 | 1.56 ± 0.88 | 2.04 ± 1.68 | 0.178 |

**Note.**— Values are presented as mean ± standard deviation ($cm^3$). LN = lymph node, ROI = regions of interest

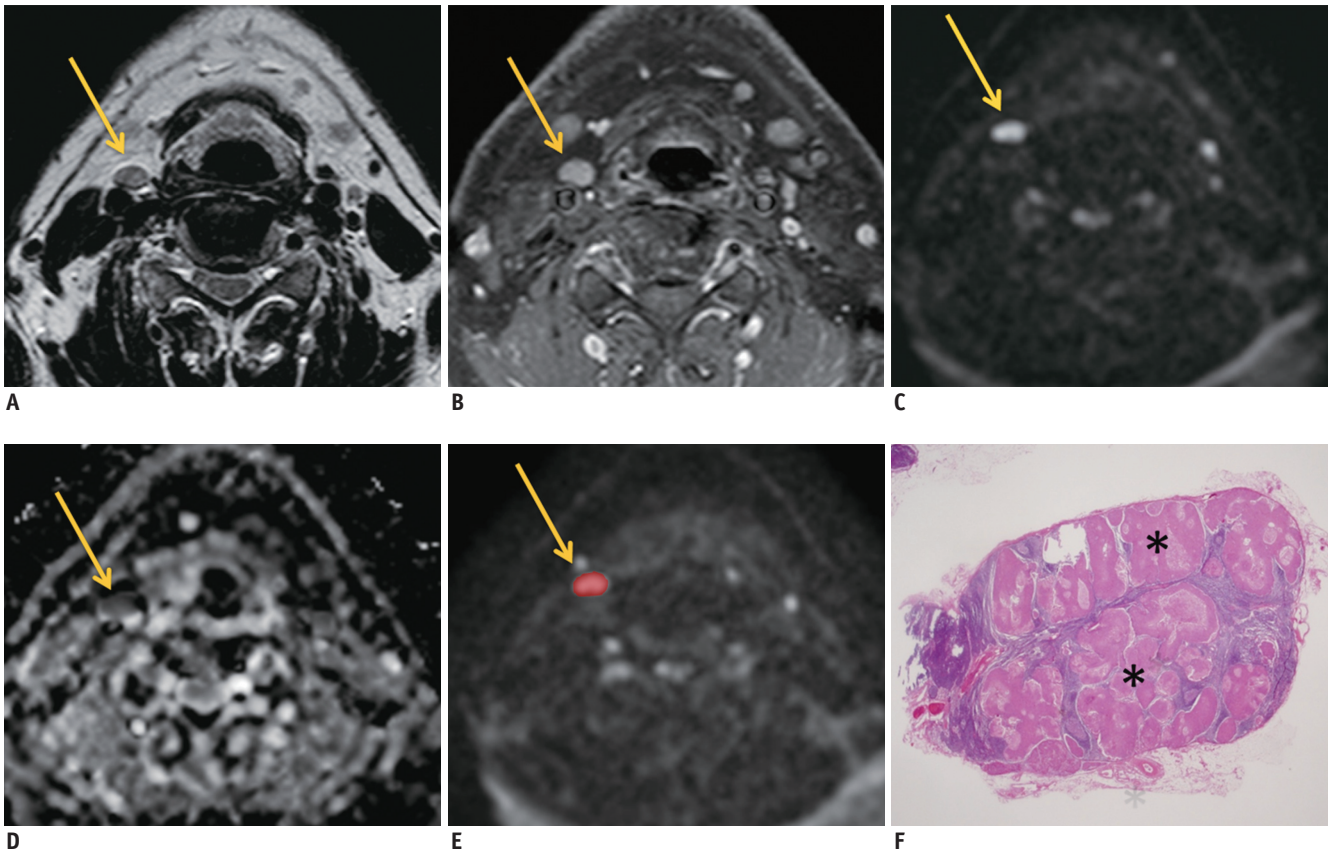


**Fig. 2. Squamous cell carcinoma of base of tongue in 69-year-old man.**
Axial T2-weighted **(A)** and gadolinium-enhanced, axial T1-weighted fat saturated **(B)** images show 6.3-mm size lymph node at right level III (arrows). This lymph node (arrows) shows high signal intensity on diffusion-weighted imaging at b = 800 $s/mm^2$ **(C)**, as well as low apparent diffusion coefficient (ADC) value on ADC map **(D)**. Regions of interest (red color) were drawn freehand over lymph node on diffusion-weighted imaging (**E**, arrow). Measured ADC value is 0.54 x $10^{-3}$ $mm^2/s$ according to reader 1 and 0.74 x $10^{-3}$ $mm^2/s$ according to reader 2, and which are under threshold for malignancy in previously published studies. On histopathologic examination **(F)**, almost all of area of this lymph node was seen to be covered with metastatic deposit (asterisk) (original magnification, x 150).

extravascular space (19). In metastatic lymph nodes from patients with HNSCC, the different environment of the water protons, such as the decreased extracellular space, increased cellularity, and higher nuclear-to-cytoplasmic ratio results in limited motion of water molecules and is represented as an area of hyperintensity on DWI acquired at a high b value of 800–1000 and low signal intensity on the corresponding ADC map. However, a diagnostic problem occurs with such a small, non-necrotic lymph node when the mean ADC value is applied to distinguish between benign and metastatic lymph nodes because of the small size of the metastatic foci within the lymph node.

In this study, we hypothesized that the percentage of metastatic foci within a small metastatic lymph node without necrosis or morphological change is relatively small and that small and dispersed metastatic deposits in an otherwise normal lymph node are less likely to create sufficient architectural change to affect the mean ADC value; thus, resulting in no significant difference in the mean ADC value compared to that of a benign lymph node. Figures 2 and 3 show representative cases of metastatic lymph nodes with relatively low and high ADC values, which support our hypothesis. Based on our results, we speculate that the mean ADC value is wide ranging due to

Korean Journal of Radiology
KJR

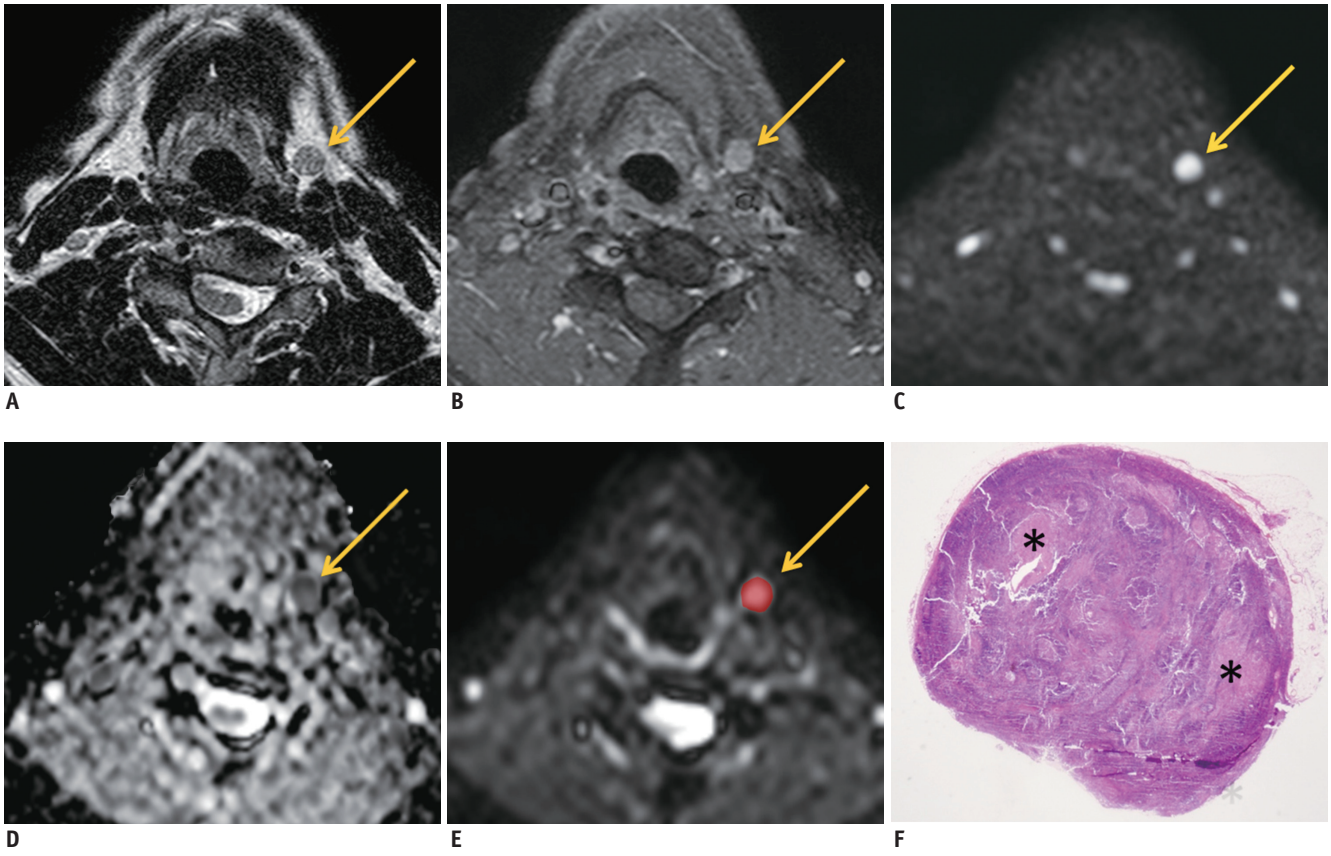


**Fig. 3. Squamous cell carcinoma of mobile tongue in 61-year-old man.**
Axial T2-weighted **(A)** and gadolinium-enhanced, axial T1-weighted fat saturated **(B)** images show 8.2-mm size lymph node at left level II (arrows). This lymph node shows high signal intensity on diffusion-weighted imaging at b = 800 s/mm$^2$ **(C)**, and high apparent diffusion coefficient (ADC) value on ADC map **(D)**. Regions of interest (red color) were drawn freehand over lymph node (**E**, arrow). Measured ADC value is 1.22 x 10$^{-3}$ mm$^2$/s according to reader 1 and 1.10 x 10$^{-3}$ mm$^2$/s according to reader 2, and which are above threshold for malignancy in previously published studies, and, therefore, are thought to be benign lymph node. However, on histopathologic examination **(F)**, partially involved metastatic foci (asterisk) are observed (original magnification, x 150).

ADC heterogeneity within the lymph node based on the proportion of metastatic infiltration within the lymph node. Considering the variability of ADC values within a lymph node, the minimum ADC value, rather than the mean ADC, might be useful to detect the smallest focal metastasis within a lymph node and serve as a better imaging marker for lymph node metastasis (20).

In contrast to our results, a study by Vandecaveye et al. (9) reported that even in subcentimeter node analysis, the ADC values of metastatic lymph nodes were significantly lower than those of benign lymph nodes, and DWI had higher sensitivity for distinguishing benign from metastatic lymph nodes. This difference from our study might be attributed to a difference in DWI parameters including b values and the numbers of patients enrolled. The b value used in our study was slightly lower than that of Vandecaveye's. We chose the highest b value of 800 s/mm$^2$ to obtain images with less susceptibility to artifacts and a higher signal-to-noise ratio.

Our study had several limitations. First, it was retrospective. To overcome this limitation, we carefully included lymph nodes without morphologically malignant criteria according to the consensus of two readers, as well as a relatively homogeneous patient group (only squamous cell carcinoma). Second, because of the retrospective design, complete topographic matching of lymph nodes between MRI and the pathological specimens was impossible. Third, there was a potential limitation when drawing the ROIs for small lymph nodes. However, this limitation made no significant difference in our study based on the results of the inter-observer variation regarding ROI volumes and ADC values between the two readers. Fourth, because DWIs were obtained with two MRI scanners with different magnetic field strengths (1.5-T vs. 3-T), different spatial resolution between the two machines may have influenced the ADC values. Last, the number of metastatic lymph nodes included was relatively small. Further

large-scale studies are necessary to confirm our results. Regardless of these limitations, the strength of our study was that we excluded enlarged and necrotic lymph nodes, which was different from previous studies. As a result, we were free from a potential interpretation bias based on morphological criteria.

In conclusion, we found that mean ADC values were not different between benign and metastatic cervical lymph nodes of small size and non-necrotic appearance in patients with HNSCC, suggesting that DWI is of no additional value for morphological criteria such as size or central necrosis. Future research is required that focuses on detailed assessment methods such as voxel distribution analysis of the ADC value, particularly to detect small metastatic foci within normal lymph nodes.

## REFERENCES

1. van den Brekel MW, Stel HV, Castelijns JA, Nauta JJ, van der Waal I, Valk J, et al. Cervical lymph node metastasis: assessment of radiologic criteria. *Radiology* 1990;177:379-384
2. van den Brekel MW, Castelijns JA, Snow GB. The size of lymph nodes in the neck on sonograms as a radiologic criterion for metastasis: how reliable is it? *AJNR Am J Neuroradiol* 1998;19:695-700
3. Yuasa K, Kawazu T, Nagata T, Kanda S, Ohishi M, Shirasuna K. Computed tomography and ultrasonography of metastatic cervical lymph nodes in oral squamous cell carcinoma. *Dentomaxillofac Radiol* 2000;29:238-244
4. King AD, Tse GM, Ahuja AT, Yuen EH, Vlantis AC, To EW, et al. Necrosis in metastatic neck nodes: diagnostic accuracy of CT, MR imaging, and US. *Radiology* 2004;230:720-726
5. Som PM. Detection of metastasis in cervical lymph nodes: CT and MR criteria and differential diagnosis. *AJR Am J Roentgenol* 1992;158:961-969
6. van den Brekel MW. Lymph node metastases: CT and MRI. *Eur J Radiol* 2000;33:230-238
7. Ng SH, Yen TC, Chang JT, Chan SC, Ko SF, Wang HM, et al. Prospective study of [18F]fluorodeoxyglucose positron emission tomography and computed tomography and magnetic resonance imaging in oral cavity squamous cell carcinoma with palpably negative neck. *J Clin Oncol* 2006;24:4371-4376
8. Troost EG, Vogel WV, Merkx MA, Slootweg PJ, Marres HA, Peeters WJ, et al. 18F-FLT PET does not discriminate between reactive and metastatic lymph nodes in primary head and neck cancer patients. *J Nucl Med* 2007;48:726-735
9. Vandecaveye V, De Keyzer F, Vander Poorten V, Dirix P, Verbeken E, Nuyts S, et al. Head and neck squamous cell carcinoma: value of diffusion-weighted MR imaging for nodal staging. *Radiology* 2009;251:134-146
10. Sumi M, Sakihama N, Sumi T, Morikawa M, Uetani M, Kabasawa H, et al. Discrimination of metastatic cervical lymph nodes with diffusion-weighted MR imaging in patients with head and neck cancer. *AJNR Am J Neuroradiol* 2003;24:1627-1634
11. Abdel Razek AA, Soliman NY, Elkhamary S, Alsharaway MK, Tawfik A. Role of diffusion-weighted MR imaging in cervical lymphadenopathy. *Eur Radiol* 2006;16:1468-1477
12. de Bondt RB, Hoeberigs MC, Nelemans PJ, Deserno WM, Peutz-Kootstra C, Kremer B, et al. Diagnostic accuracy and additional value of diffusion-weighted imaging for discrimination of malignant cervical lymph nodes in head and neck squamous cell carcinoma. *Neuroradiology* 2009;51:183-192
13. Holzapfel K, Duetsch S, Fauser C, Eiber M, Rummeny EJ, Gaa J. Value of diffusion-weighted MR imaging in the differentiation between benign and malignant cervical lymph nodes. *Eur J Radiol* 2009;72:381-387
14. Perrone A, Guerrisi P, Izzo L, D'Angeli I, Sassi S, Mele LL, et al. Diffusion-weighted MRI in cervical lymph nodes: differentiation between benign and malignant lesions. *Eur J Radiol* 2011;77:281-286
15. Jansen JF, Stambuk HE, Koutcher JA, Shukla-Dave A. Non-gaussian analysis of diffusion-weighted MR imaging in head and neck squamous cell carcinoma: a feasibility study. *AJNR Am J Neuroradiol* 2010;31:741-748
16. King AD, Ahuja AT, Yeung DK, Fong DK, Lee YY, Lei KI, et al. Malignant cervical lymphadenopathy: diagnostic accuracy of diffusion-weighted MR imaging. *Radiology* 2007;245:806-813
17. Wu LM, Xu JR, Liu MJ, Zhang XF, Hua J, Zheng J, et al. Value of magnetic resonance imaging for nodal staging in patients with head and neck squamous cell carcinoma: a meta-analysis. *Acad Radiol* 2012;19:331-340
18. Gallus J, Mathiowetz V. Test-retest reliability of the Purdue Pegboard for persons with multiple sclerosis. *Am J Occup Ther* 2003;57:108-111
19. Koh DM, Collins DJ. Diffusion-weighted MRI in the body: applications and challenges in oncology. *AJR Am J Roentgenol* 2007;188:1622-1635
20. Lee SC, Moon WJ, Choi JW, Roh HG, Bak SH, Yi JG, et al. Differentitation between primary central nervous system lymphoma and glioblastoma: added value of quantitative analysis of CT attenuation and apparent diffusion coefficient. *J Korean Soc Magn Reson Med* 2012;16:226-235